

Effect of inelastic scattering on the resonance line shapes in He-graphite

James S. Hutchison*

Department of Physics, University of Virginia, Charlottesville, Virginia 22901

(Received 12 May 1980)

Recent experiments on the scattering of low-energy neutral helium beams from the basal surface of graphite have produced detailed spectra with prominent resonant features characteristic of physisorption of the incident atoms. Elastic calculations of the expected angular spectra show only qualitative agreement, with large discrepancies in both the overall scattered intensity and the widths and, in some cases, the signatures of the resonances. By consistently including a Debye-Waller factor to account for inelastic processes in scattering from the strongly repulsive part of the atom-surface potential, we obtain calculated spectra in very good agreement with observation, except near grazing incidence.

I. INTRODUCTION

The kinematics of selective adsorption phenomena in atom-surface scattering was elucidated long ago by Lennard-Jones and Devonshire. In recent years, the quality of experimental spectra has increased markedly, and several systems have been characterized in sufficient detail to allow meaningful comparison to dynamical theories. Elastic calculations for helium scattered from the (01) surface of LiF (Refs. 1 and 2) have shown detailed agreement with the observed resonance structure, if the predicted overall scattered intensity is multiplied by a Debye-Waller factor of about 0.3. Similar calculations for the He-graphite (0001) system have not been as successful,³ and a detailed comparison with experiment⁴ shows the predicted resonance structures to be both very narrow and too intense, with a particular "closed-channel" resonance having the wrong shape (see Fig. 1 of this paper). The atom-surface potential for this system is thought to be rather well characterized from the kinematics of the scattering, the band structure of physisorbed helium,^{5,6} and thermodynamic data; semiempirical calculations⁷ are consistent with this potential. The observed discrepancies were ascribed to inelastic processes in the above report³ and an optical potential⁸ was employed to demonstrate that these effects can produce the requisite softening and broadening of an isolated adsorption resonance.

We have recently presented⁹ a general theory for resonant atom-surface scattering which assumes the atom-surface potential to be the composite of a corrugated short-range repulsion and a laterally smooth long-range attraction, and have applied approximate methods to discuss the qualitative features of adsorption resonances. This formulation is not limited to approximate considerations, however, and provides a flexible frame-

work for quantitative calculation. By including a Debye-Waller attenuation for scattering from the repulsive part of the potential, the strongest inelastic effects can be incorporated in a natural way with remarkably good results. The purpose of this paper is twofold: To demonstrate a calculation procedure for a realistic atom-surface potential that does not require massive computation, and to display results for the He-graphite system which include inelastic effects in other than a phenomenological manner.

A short review of the general theory is provided in the next section. Section III details the explicit calculation procedures and Sec. IV displays the results and provides a discussion thereof.

II. GENERAL PROCEDURE

We apply the theory of Ref. 9 and employ the same notation. The procedure is as follows:

(i) For each momentum (\vec{k}_0, k_{0z}) of the incident atom, preselect the reciprocal lattice vectors \vec{F} which lead to diffracted beams of interest and the reciprocal lattice vectors \vec{N} which are such that $2mD > p_N^2 > 0$. Here D is the depth of the attractive well and $p_N^2 = 2m(E_0 + D) - (\vec{k}_0 + \vec{N})^2$ with E_0 incident energy.

(ii) Compute the scattering amplitudes $S(\vec{F}, \vec{0})$, $S(\vec{0}, \vec{F})$, $S(\vec{N}, \vec{0})$, $S(\vec{0}, \vec{N})$, and $S(\vec{N}, \vec{N}')$ for reflection and diffraction from the repulsive part of the potential at energy $E_0 + D$. The relevant processes connect the initial beam ($\vec{0}$) to the final beams (\vec{F}) and to the beams in the well (\vec{N}), and the latter to each other.

(iii) Characterize the attractive well by a phase shift δ as a function of the perpendicular energy $\epsilon = (p^2/2m) - D$. Actually δ is needed only for $p = p_N$ and $e^{i\delta_N}$ is then denoted by R_N .

(iv) Solve for X_N the equations

$$\sum_{N'} [\delta_{NN'} - R_N S(\vec{N}, \vec{N}')] X_{N'} = R_N S(\vec{N}, \vec{0}) \quad (2.1)$$

and compute the total scattering intensities

$$\frac{k_{F\mathbf{k}}}{k_{0\mathbf{k}}} |A_F|^2 = \frac{p_F}{p_0} \left| \sum_N S(\vec{F}, \vec{N}) X_N + S(\vec{F}, \vec{0}) \right|^2. \quad (2.2)$$

In the notation of Ref. 9, $X_N = B_N^* R_N / T_0'$ with $|T_0'|^2 = k_{0\mathbf{k}} / p_0$. It should be noted that Eqs. (2.1) represent a unitary approximation, i.e., these elastic intensities obey

$$\sum_F \frac{k_{F\mathbf{k}}}{k_{0\mathbf{k}}} |A_F|^2 = 1, \quad (2.3)$$

provided that the matrix S is unitary. The method for obtaining values of S as well as the phase shifts that characterize the reflection coefficients R_N requires specification of the potential and is detailed in the next section. The scattered intensities are then obtained simply by inverting (2.1) (which in our case involved at most a 12×12 matrix, although usually a smaller number of \vec{N} vectors are in fact important) and performing the required sums.

The intensities obtained from the elastic theory, however, do not adequately describe the resonance structure seen in the He-graphite system. The failure is not due to possible inadequacies of the potential used, and cannot be remedied even by the introduction of an *ad hoc* optical potential. In the present formalism, however, the effect of inelastic processes on resonances can be included in a straightforward way as discussed below.

For scattering from a hard surface where the collision process is of short duration compared to a relevant phonon frequency, Levi and Suhl¹⁰ have shown the elementary Debye-Waller attenuation to hold for two opposite limits: Completely correlated and completely uncorrelated motions of the surface. A similar result was previously described by Duke and Laramore¹¹ who obtained a "square root of a Debye-Waller factor" as the leading correction to each interaction vertex in their general perturbation expansion for particle-surface scattering. To incorporate the strongest inelastic effects into the theory presented above we make the following replacement for all the "hard-wall" amplitudes:

$$S(\vec{G}, \vec{G}') \rightarrow e^{-W(\vec{G}, \vec{G}')} S(\vec{G}, \vec{G}'), \quad (2.4)$$

where the exponent

$$W(\vec{G}, \vec{G}') = \frac{1}{2} \langle u_{\mathbf{k}}^2 \rangle (p_G + p_{G'})^2 / \hbar^2 \quad (2.5)$$

naturally contains the Beeby correction,¹² i.e., the momentum transfer corresponds to the energy computed from the bottom of the potential well. Only the large perpendicular momentum transfer has been included, and corresponding only the perpendicular component of the surface displacement appears in the thermally averaged $\langle u_{\mathbf{k}}^2 \rangle$.

III. ATOM-SURFACE POTENTIAL

For the calculation presented here, the repulsive potential is assumed to be $V_r(z - \zeta(\vec{R}))$, with

$$\zeta(\vec{R}) = \sum_G \zeta_G e^{i\vec{G} \cdot \vec{R}}, \quad (3.1)$$

where V_r is an infinite step ("hard wall") and the corrugation $\zeta(\vec{R})$ is limited to first-order reciprocal lattice vectors. This choice is strongly indicated by the previous successes^{1,2} of this model for alkali-halide surfaces and for the observed intensities¹³ of diffracted orders for He-graphite, which fix $\zeta_{10} = -0.023 \text{ \AA}$ largely independent of incident energy. The scattering matrix elements for such a hard-wall potential have been investigated thoroughly.¹⁴ For a sinusoidal corrugation, the most convenient method¹⁵ is to solve Rayleigh's equations by expanding in the corrugation parameter. The recursive series obtained is easy to implement numerically and converges rapidly for the relatively smooth graphite surface and the low energies here considered.

The phase shift δ that characterizes reflection from the attractive potential can be obtained by direct integration of the one-dimensional Schrödinger equation for some model potential.¹⁶ A more flexible technique is to obtain δ directly from an interpolation of the experimental energy eigenvalues. For a potential of the form¹⁷

$$V(z) = D[(1 + \lambda z / \eta)^{-2n} - 2(1 + \lambda z / \eta)^{-n}] \quad (3.2)$$

the eigenvalues are well approximated by

$$E_n = -D[1 - (2n + 1)\hbar\lambda / (2mD\alpha^2)^{1/2}]^\alpha, \quad (3.3)$$

where α is related to η by gamma functions,

$$\alpha(\eta) = \frac{2^{(1-1/\eta)}}{\pi^{1/2}} \frac{\Gamma\left(\frac{1}{2} - \frac{1}{\eta}\right)}{\Gamma\left(2 - \frac{1}{\eta}\right)}. \quad (3.4)$$

The three adjustable parameters D , α , and η fix the depth, range, and "steepness" or asymmetry of the potential, respectively. Values for these parameters are obtained by fitting the kinematics of the observed bound-state resonances⁴ to the eigenvalue equation (3.3). The desired reflection amplitudes are obtained by considering Eq. (3.3) a function of the continuous variable n and inverting for arbitrary energy ϵ ($\epsilon < 0$):

$$n(\epsilon) = \frac{(2mD)^{1/2}\alpha}{2\hbar\lambda} \left[1 - \left(-\frac{\epsilon}{D} \right)^{1/\alpha} \right] - \frac{1}{2}. \quad (3.5)$$

For an allowed value of $\epsilon = (p_N^2/2m) - D$ we define $\delta_N = 2\pi n(\epsilon_N)$, and identify δ_N as the phase accrued during one period of oscillation in the potential. Comparison with the definition of R_N in Eq. (2.1) shows that indeed $R_N = e^{i\delta_N}$, provided that the

phase of $S(\vec{N}, \vec{N})$ is chosen so that $S(\vec{N}, \vec{N}) = 1$ for a flat surface.

In Ref. (9) δ_N was defined as the phase of $R_N S(\vec{N}, \vec{N})$. In many interesting cases (weak corrugation, as in graphite, or sinusoidal corrugation on a square lattice, as in LiF) the two definitions agree. Even when the phase of $S(\vec{N}, \vec{N})$ cannot be neglected, it varies slowly with energy, so that formulas involving $d\delta/d\epsilon$ [e.g., (4.2) below] are unaffected. In general, however, $R_N = 1$ gives the bound states of the laterally averaged potential, while the bound-state resonances are determined by the phase of $R_N S(\vec{N}, \vec{N})$.

IV. RESULTS

Experiments by Boato *et al.*⁴ provide a detailed picture of both the specular [$\vec{F} = (0, 0)$] intensity and the $\vec{F} = (\vec{1}, 0)$ diffracted intensity for an incident wave vector $k_0 = 6.49 \text{ \AA}^{-1}$. By fitting the reported bound-state spectrum to Eq. (3.3), the values for the potential parameters were found to be $D = 15.8 \text{ meV}$, $\lambda = 1.45 \text{ \AA}^{-1}$, and $\alpha = 3.12$, which corresponds roughly to a 10^{-5} interaction potential. This choice yields five bound states which are consistent with the data within the reported experimental uncertainty. By using a helium-cooled nozzle source, Wesner *et al.*¹⁸ have extended these investigations of the specular intensity to lower energies, specifically $k_0 = 5.67, 4.31, \text{ and } 3.12 \text{ \AA}^{-1}$. Using the potential fixed by the parameters above we have investigated these four scattering energies.

The calculated elastic intensities [labeled (b)] are displayed in Figs. 1–4 along with the corresponding experimental intensities [labeled (a)]. The plots labeled (c) include the inelastic effects according to Eq. (3.8). The value of $\langle u_z^2 \rangle = (0.065 \text{ \AA})^2$, arbitrarily chosen to match the background intensity in Fig. 1(a) at $\theta_i = 30^\circ$, corresponds to the zero-point motion for a Debye solid with a Debye temperature of 750 K. This value coincides with the best independent estimates¹⁹ for the surface Debye temperature of graphite. For the surface temperature of about 100 K reported for all these experiments there should be no appreciable dependence of $\langle u_z^2 \rangle$ upon possible small temperature variations and the same value was used throughout.

Examination of the calculated elastic intensities reveals large deviations from experiment in both the overall background intensity and the details of the resonant structure. The previous calculations³ for $k_0 = 6.49 \text{ \AA}^{-1}$ using a slightly different potential give results nearly identical to Fig. 1(b); many of the deficiencies of the elastic calculation are catalogued in Ref. 3. The Debye-Waller correction

included in Figs. 1(c)–4(c) is seen to provide much general improvement in the calculated spectrum, and several details are of particular interest.

Certain resonance features (marked by asterisks in Figs. 1–4) are seen to change from small maxima to strong minima due to the inelasticity. Analysis of the kinematics shows these to be “closed-channel” resonances—the bound state is coupled strongly (meaning via a first-order diffraction) to only the specular beam and to no other free diffraction channel.²⁰ Because the other free channels are hardly affected, the flux conservation condition [Eq. (2.3)] requires the effect of these resonances upon the specular intensity to be correspondingly small. The effect is clearly displayed by the approximate solution⁹ to Eqs. (2.1) valid near an isolated resonance. Keeping only one N channel one obtains

$$|A_0|^2 = |S(\vec{0}, \vec{N})R_N S(\vec{N}, \vec{0})[1 - R_N S(\vec{N}, \vec{N})]^{-1} + S(\vec{0}, \vec{0})|^2. \quad (4.1)$$

This describes a resonance with energy width²¹

$$\Gamma_N = 2 \left(|S(\vec{N}, \vec{N})| \frac{d\delta_N}{d\epsilon} \right)^{-1} [1 - |S(\vec{N}, \vec{N})|]. \quad (4.2)$$

For elastic scattering, the unitarity of S constrains the ratio of the first (resonant) term to the second (direct) term in Eq. (4.1) to be close to -2 at resonance, since $S(\vec{0}, \vec{0}) \approx 1$ and

$$S(\vec{N}, \vec{N}) \approx [1 - S(\vec{0}, \vec{N})S(\vec{N}, \vec{0})]^{1/2} \approx 1 - \frac{1}{2}S(\vec{0}, \vec{N})S(\vec{N}, \vec{0}),$$

hence the closed-channel resonance is nearly invisible. For the graphite surface $|S(\vec{N}, \vec{N})|$ is typically 0.9 or larger, and including the Debye-Waller attenuation can increase the resonance width by a factor of 5 or more. This is the dominant inelastic effect in this case: The modulus of the resonant term is correspondingly decreased, destroying the balance of the resonant to direct terms and producing the observed minimum. Such closed-channel features, present for all the energies considered, provide a good test for the theory. While any inelastic scaling, for instance employing an optical potential,²⁰ produces the desired change from maximum to minimum simply from unitarity considerations, the strengths of these resonances are very sensitive to the amount to inelastic scattering. The correct behavior of these features for the various energies reported supports the validity of the Debye-Waller attenuation.

Examination of Eqs. (4.1) and (4.2) also provides an explanation for the relative success of the purely elastic theory in reproducing the observed resonance structure for He-LiF at comparable energies. The inelastic reduction in overall intensity

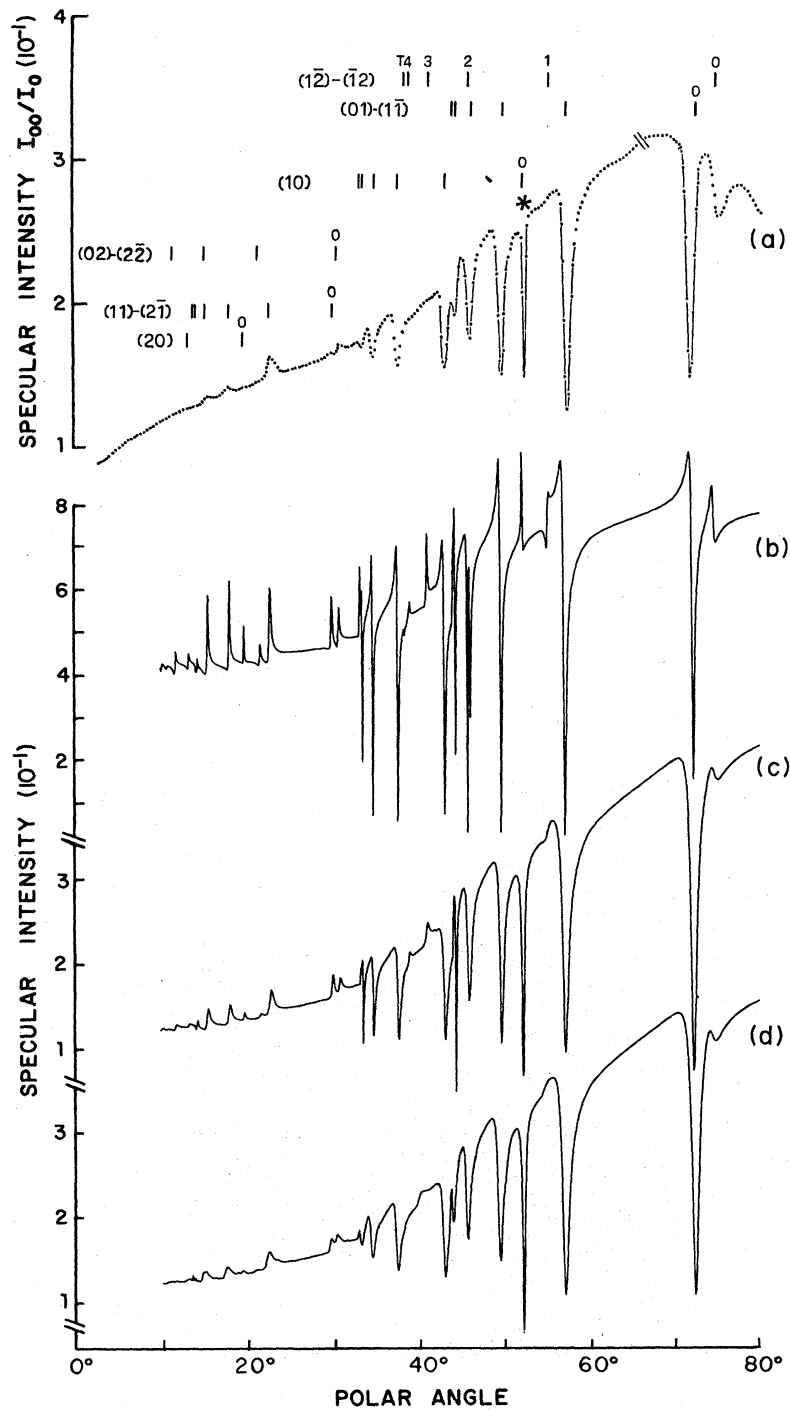


FIG. 1. Specular scattering of 22-meV helium atoms from the basal surface of graphite. The intensity observed by Boato *et al.* (Ref. 4) is reproduced in panel (a) with the other panels calculated as follows: (b) elastic theory, (c) Debye-Waller attenuation, and (d) Debye-Waller attenuation and convolution with the energy dispersion of the experimental beam. The resonance features are labeled according to the diffraction order and the energy level of the laterally averaged potential. The asterisks indicate a channel strongly coupled only to the specular beam as discussed in Sec. IV.

for the two systems is approximately the same, hence one would expect a similar Debye-Waller scaling. For He-LiF, however, the surface corrugation is larger than for He-graphite by a factor of 3 (Ref. 2) and the diagonal matrix elements $|S(\vec{N}, \vec{N})|$ typically have values of 0.6. The resonance widths and the balance between resonant and

direct terms are therefore much less sensitive to the effects of inelasticity.

The spectrum of Fig. 1(c), for instance, still contains narrow features not reflected in the experiment, which can be identified with bound states close to the continuum threshold. As is seen from Eq. (4.2), the energy width of a resonance is pro-

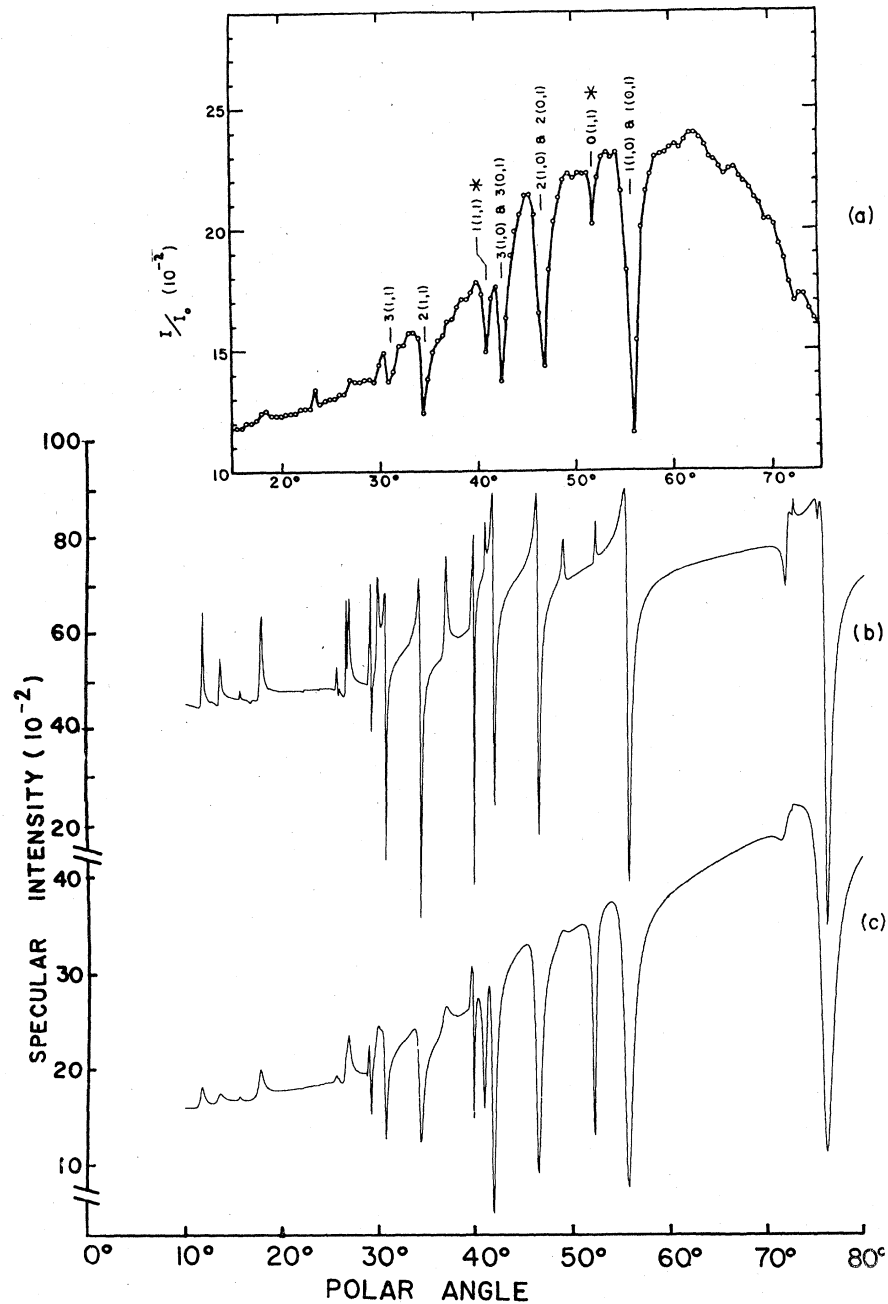


FIG. 2. Specular scattering of 16.8-meV helium atoms from the basal surface of graphite. The experimental intensities (a) are from Wesner *et al.* (Ref. 18) and the calculated spectra are as in Fig. 1 except convolution with the beam energy dispersion is omitted. Notice that the labeling convention for the reciprocal surface differs from that of Fig. 1.

portional to $(d\delta/d\epsilon)^{-1}$. This factor, inversely proportional to the energy density of states, becomes small near threshold for any long-range attractive potential. The absence of this sharp structure in the data does not indicate a fundamental flaw in the theory, however, but is caused by the experimental energy dispersion in the incident beam, as we shall now demonstrate.

If the resonance line shapes are assumed for

simplicity to be Gaussian, the observed energy width of a resonance will be

$$\Gamma_{\text{obs}}^2 = \frac{\partial \epsilon^2}{\partial k} (\Delta k)^2 + \frac{\partial \epsilon^2}{\partial \theta} (\Delta \theta)^2 + \frac{\partial \epsilon^2}{\partial \phi} (\Delta \phi)^2 + \Gamma_0^2, \quad (4.3)$$

where Γ_0 is the actual width and $\Delta \theta$, $\Delta \phi$, and Δk reflect the dispersion of the incident beam. The derivatives refer to the kinematic energy conser-

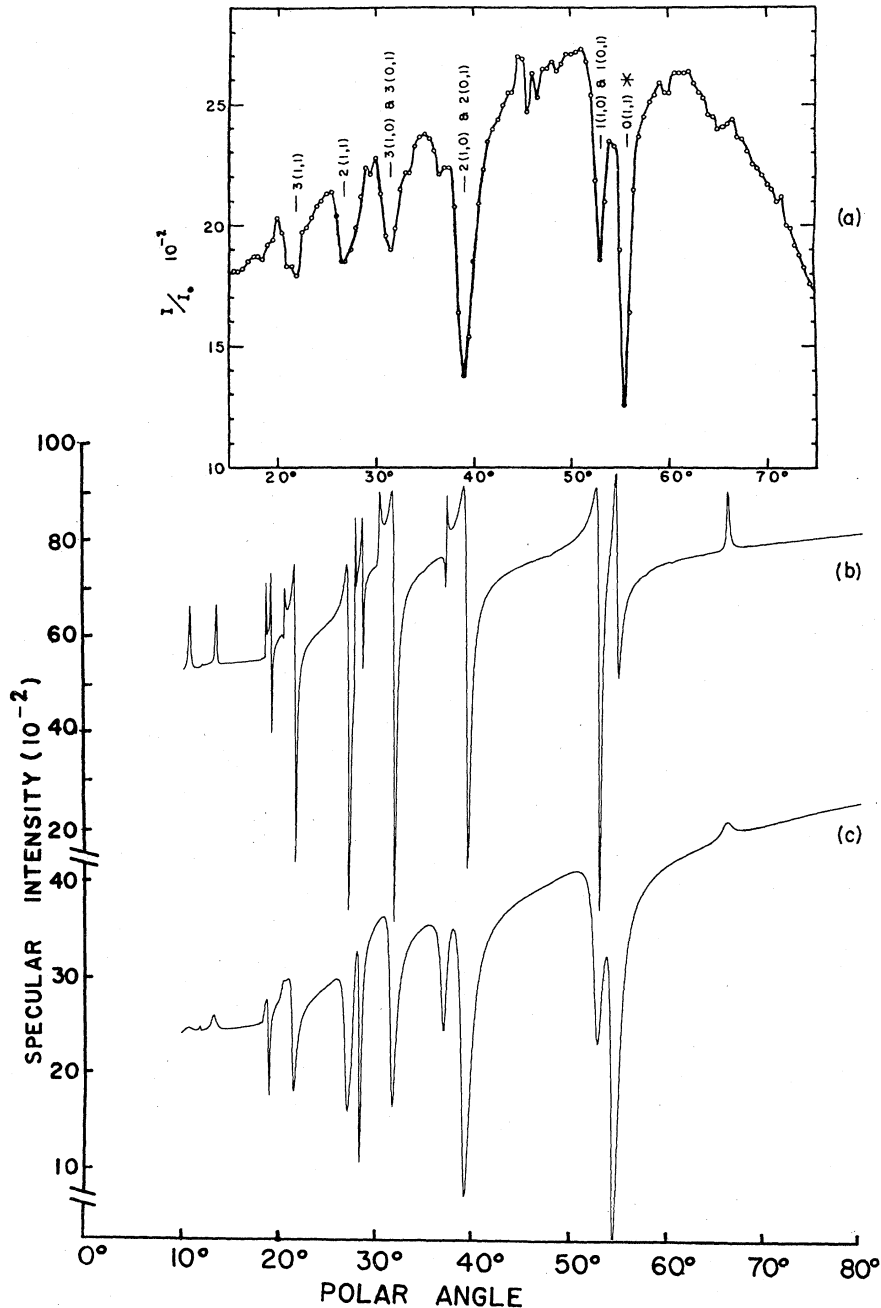


FIG. 3. Same as Fig. 2 for incident energy 9.7 meV.

vation condition

$$\epsilon = (\hbar^2/2m)[k_{0z}^2 - (\vec{k}_0 + \vec{N})^2] \quad (4.4)$$

evaluated at resonance. For the experimental conditions, $\Delta\theta \approx \Delta\phi \approx 0.15^\circ$ and $\Delta k/k \approx 0.02$, the angular spread gives a negligible contribution. The effect of the energy dispersion is significant, however, except for certain geometries where $\partial\epsilon/\partial k$ can vanish for the lower bound states. [This is

partially responsible for the narrowness of the 0-(1,0) resonance at 52° in Fig. 1(a).⁴]

The energy dispersion was incorporated into the calculated spectrum by numerically convoluting the inelastic intensity with the appropriate Gaussian distribution in incident energy. The resulting intensity, displayed in Fig. 1(d), is seen to reproduce the experiment rather well, except near grazing incidence. Thus the apparent discrepancy

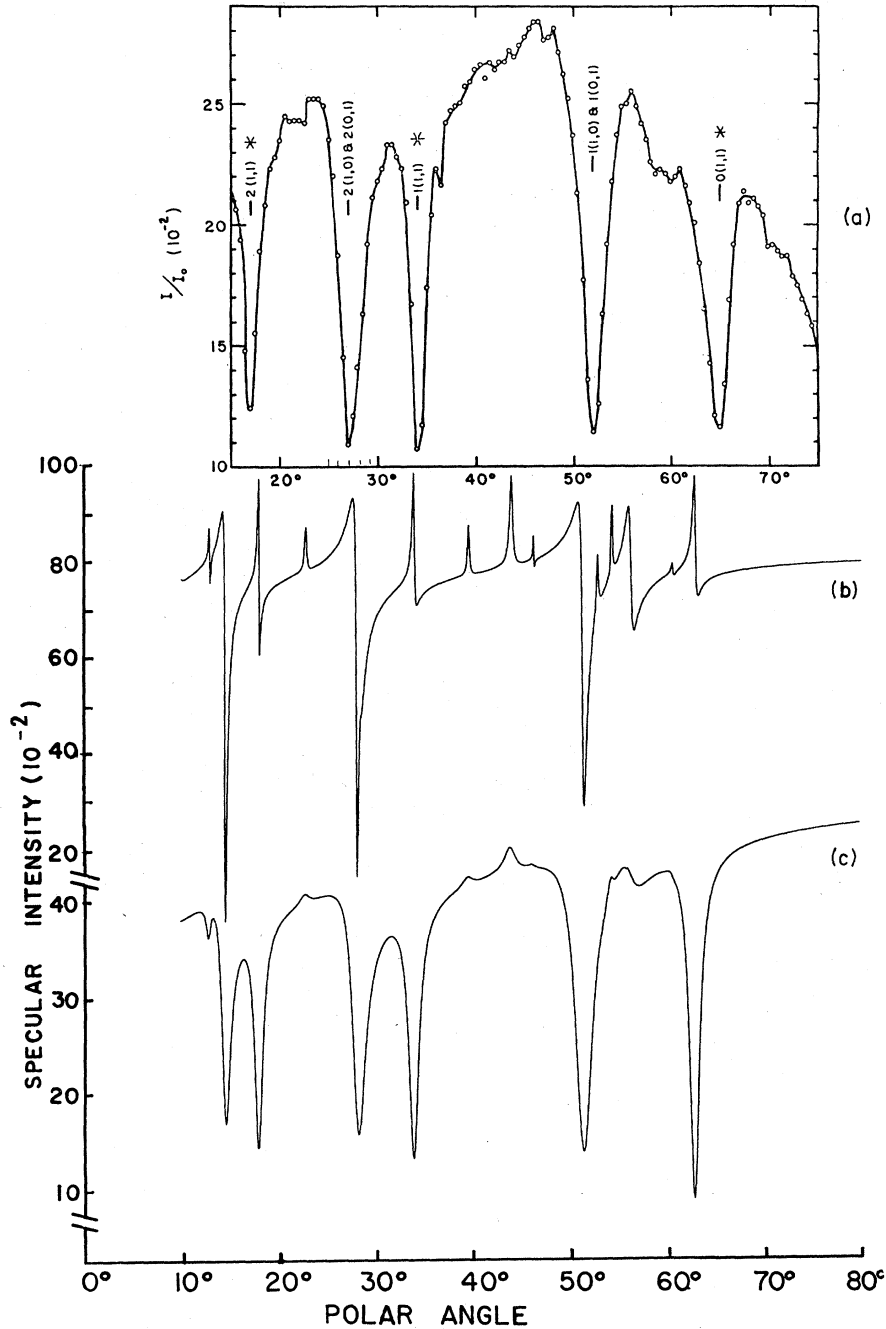


FIG. 4. Same as Fig. 2 for incident energy 5.1 meV.

between experimental and theoretical widths near the dissociation limit⁴ is probably due to the difficulty of deconvoluting theoretical widths from the data.

The remaining discrepancy between theory and experiment occurs at near-grazing incidence and is more pronounced at the lower incident energies. The sizeable drop in experimental intensity under these conditions is regarded as an experimental artifact by many, including the authors of Ref. 18, but a recent study of this question by Garcia *et al.*²² concludes that the effect is intrinsic to the atom-surface scattering. The question is very interesting since it may be connected with the increase in accommodation and sticking at low temperature,

which is not predicted by simple quantum theories. One can modify the Debye-Waller attenuation to fit the data,²² but the proposed modification lacks theoretical justification and the very success of standard Debye-Waller theory reported in this paper shows that the effect, if true, is rather subtle. Further work on this question is in progress.

ACKNOWLEDGMENTS

It is a pleasure to thank V. Celli and N. Garcia for many helpful discussions and comments, and the Genoa and Penn State groups for advance communication of their data. This work was supported in part by NSF Grant No. DMR-76-17375.

*Present address: Department of Physics, University of Maine, Orono, Maine 04469.

¹C. E. Harvie and J. H. Weare, *Phys. Rev. Lett.* **40**, 187 (1978).

²N. Garcia, V. Celli, and F. O. Goodman, *Phys. Rev. B* **19**, 1808 (1979).

³N. Garcia, W. Carlos, M. Cole, and V. Celli, *Phys. Rev. B* **21**, 1636 (1980).

⁴G. Boato, P. Cantini, C. Guidi, R. Tatarek, and G. P. Felcher, *Phys. Rev. B* **20**, 3957 (1979); G. Derry, D. Wesner, W. Carlos, and D. R. Frankl, *Surf. Sci.* **87**, 629 (1979).

⁵J. Hutchison and V. Celli, *Surf. Sci.* **93**, 263 (1980).

⁶Y. Hamauzu, *J. Phys. Soc. Jpn.* **42**, 961 (1977);

H. Chow, *Surf. Sci.* **60**, 221 (1977).

⁷W. E. Carlos and M. W. Cole, *Phys. Rev. Lett.* **43**, 697 (1979).

⁸H. Chow and E. D. Thompson, *Surf. Sci.* **82**, 1 (1979).

⁹V. Celli, N. Garcia, and J. Hutchison, *Surf. Sci.* **87**, 112 (1979).

¹⁰A. C. Levi and H. G. Suhl (unpublished).

¹¹C. B. Duke and G. E. Laramore, *Phys. Rev. B* **2**, 4765

(1970).

¹²J. L. Beeby, *J. Phys. C* **4**, L359 (1971).

¹³G. Boato, P. Cantini, and R. Tatarek, *Phys. Rev. Lett.* **40**, 887 (1978).

¹⁴G. Armand and J. R. Manson, *Phys. Rev. B* **19**, 4091 (1979).

¹⁵C. Lopez, F. J. Yndurain, and N. Garcia, *Phys. Rev. B* **18**, 970 (1978); see also Ref. 1.

¹⁶N. Garcia, Frank O. Goodman, V. Celli, and N. R. Hill, *Phys. Rev. B* **19**, 1808 (1979).

¹⁷E. Ghio, L. Mattera, C. Salvo, F. Tommasini, and U. Valbusa, *J. Chem. Phys.* (in press).

¹⁸D. Wesner, G. Derry, G. Vidali, T. Thwaites, and D. R. Frankl, *Surf. Sci.* **95**, 367 (1980).

¹⁹J. P. Biberian, M. Bienfait, and J. B. Theeten, *Acta Crystallogr. Sect. A* **29**, 221 (1973).

²⁰K. L. Wolfe and J. H. Weare, *Surf. Sci.* **94**, 581 (1980).

²¹The result quoted in Ref. 9 is strictly correct only for elastic scattering in the weakly corrugated limit where $|S|$ is close to 1.

²²N. Garcia, L. Greiner, H. Hoinkes, and H. Wilsch, *Surf. Sci.* (in press).